


RESEARCH ARTICLE

Immunohistochemistry and oxygen saturation endoscopic imaging reveal hypoxia in submucosal invasive esophageal squamous cell carcinoma

Nobuhisa Minakata^{1,2}  | Shingo Sakashita³ | Masashi Wakabayashi⁴ | Yuka Nakamura⁵ | Hironori Sunakawa^{1,6} | Yusuke Yoda^{1,7} | Genichiro Ishii^{2,8} | Tomonori Yano^{1,2,6}

¹Department of Gastroenterology and Endoscopy, National Cancer Center Hospital East, Kashiwa, Japan

²Course of Advanced Clinical Research of Cancer, Juntendo University Graduate School of Medicine, Bunkyo-ku, Japan

³Division of Pathology, Exploratory Oncology Research and Clinical Trial Center, National Cancer Center, Kashiwa, Japan

⁴Biostatistics Division, Center for Research Administration and Support, National Cancer Center, Kashiwa, Japan

⁵Department of Strategic Programs, Exploratory Oncology Research and Clinical Trial Center, National Cancer Center, Kashiwa, Japan

⁶NEXT Medical Device Innovation Center, National Cancer Center Hospital East, Kashiwa, Japan

⁷Department of Gastroenterology and Endoscopy, Saitama Cancer Center, Saitama, Japan

⁸Department of Pathology and Clinical Laboratories, National Cancer Center Hospital East, Kashiwa, Japan

Correspondence

Tomonori Yano, Department of Gastroenterology and Endoscopy, National Cancer Center Hospital East, 6-5-1, Kashiwanoha, Kashiwa, Chiba 277-8577, Japan.

Email: toyano@east.ncc.go.jp

Shingo Sakashita, Division of Pathology, Exploratory Oncology Research and Clinical Trial Center, National Cancer Center, 6-5-1, Kashiwanoha, Kashiwa, Chiba 277-8577, Japan.

Email: ssakashi@east.ncc.go.jp

Funding information

Japan Society for the Promotion of Science, Grant/Award Number: JP20K22859 and JP21K06899; National Cancer Center Research and Development Fund, Grant/Award Number: 2020-A-10; Center of New Surgical and Endoscopic Development for Exploratory Technology

Abstract

Background: Hypoxic microenvironment is prominent in advanced esophageal squamous cell carcinoma (ESCC). However, it is unclear whether ESCC becomes hypoxic when it remains in the mucosal layer or as it invades the submucosal layer. We aimed to investigate whether intramucosal (Tis-T1a) or submucosal invasive (T1b) ESCC becomes hypoxic using endoscopic submucosal dissection samples.

Methods: We evaluated the expression of hypoxia markers including hypoxia inducible factor 1 α (HIF-1 α), carbonic anhydrase IX (CAIX), and glucose transporter 1 (GLUT1) by H-score and vessel density by microvessel count (MVC) and microvessel density (MVD) for CD31 and α -smooth muscle actin (α -SMA) with immunohistochemical staining ($n = 109$). Further, we quantified oxygen saturation (StO₂) with oxygen saturation endoscopic imaging (OXEI) ($n = 16$) and compared them to non-neoplasia controls, Tis-T1a, and T1b.

Results: In Tis-T1a, cccIX (13.0 vs. 0.290, $p < 0.001$) and GLUT1 (199 vs. 37.6, $p < 0.001$) were significantly increased. Similarly, median MVC (22.7/mm² vs. 14.2/mm², $p < 0.001$) and MVD (0.991% vs. 0.478%, $p < 0.001$) were markedly augmented. Additionally, in T1b, the mean expression of HIF-1 α (16.0 vs. 4.95, $p < 0.001$), CAIX (15.7 vs. 0.290, $p < 0.001$), and GLUT1 (177 vs. 37.6, $p < 0.001$) were significantly heightened, and median MVC (24.8/mm² vs. 14.2/

This is an open access article under the terms of the [Creative Commons Attribution](https://creativecommons.org/licenses/by/4.0/) License, which permits use, distribution and reproduction in any medium, provided the original work is properly cited.

© 2023 The Authors. *Cancer Medicine* published by John Wiley & Sons Ltd.

mm², $p < 0.001$) and MVD (1.51% vs. 0.478%, $p < 0.001$) were markedly higher. Furthermore, OXEI revealed that median StO₂ was significantly lower in T1b than in non-neoplasia (54% vs. 61.5%, $p = 0.00131$) and tended to be lower in T1b than in Tis-T1a (54% vs. 62%, $p = 0.0606$).

Conclusion: These results suggest that ESCC becomes hypoxic even at an early stage, and is especially prominent in T1b.

KEYWORDS

blood vessel, endoscopy, esophageal squamous cell carcinoma, hypoxia, neoplasm invasion

1 | INTRODUCTION

In advanced solid cancers, it is known that the abnormal growth of cancer cells and incomplete angiogenesis can lead to tumor hypoxia.^{1–3} In the absence of oxygen, hypoxia inducible factor 1 α (HIF-1 α), which is the hypoxic response factor, remains stable, activating the expression of hypoxia response genes, such as carbonic anhydrase IX (CAIX),⁴ glucose transporter 1 (GLUT1),⁵ vascular endothelial growth factor (VEGF),^{3,6,7} erythropoietin (EPO),³ transforming growth factor beta 3 (TGF- β 3),³ and so on. This leads to further angiogenesis, tumor invasion, and metastasis, resulting in a poor prognosis.^{2–5,8} As a result of angiogenesis, the density and number of blood vessels increase in the tumor.^{3,9,10}

Esophageal squamous cell carcinoma (ESCC) is one of the tumors that becomes hypoxic as it progresses, which leads to angiogenesis. It has a poor prognosis and high mortality rate.^{9–19} In non-neoplastic esophageal tissues, the expression of hypoxia markers such as HIF-1 α , CA9, and GLUT1 is rare,^{20–22} but in ESCC, this expression increases as it invades deeper, and the high expression of hypoxia markers is associated with a poor prognosis.^{10,12–17}

In superficial esophageal squamous cell carcinoma (SESCC), it has been reported that the expression of hypoxia markers is higher than that in non-neoplasia^{20–22} and lower than that in advanced ESCC.^{10,12–17} Furthermore, oxygen saturation endoscopic imaging (OXEI, FUJIFILM, Tokyo) collaboratively developed by our group, for visualizing the oxygen status of digestive tract lesions as a color map in real time^{23–25} has previously revealed that the oxygen saturation (StO₂) in esophageal neoplasia was significantly lower than that in non-neoplasia.²³ This finding is consistent with previous reports relating to the expression of hypoxia markers.^{10,12–17,20–22}

Recent literature suggests that ESCC is hypoxic at an early stage. However, there have been no reports comparing the oxygen status of non-neoplasia, high-grade dysplasia (pTis), intramucosal carcinoma (pT1a), and submucosal carcinoma (pT1b). Further, it is also unknown

whether ESCC is hypoxic when it remains in the mucosal layer or whether it becomes hypoxic as it invades the submucosal layer.

The aim of this study was therefore to investigate whether ESCC becomes hypoxic in pTis-T1a or pT1b by comparing the expression of hypoxia markers, vessel density, and the StO₂ with OXEI in non-neoplasia, pTis-T1a, and pT1b, respectively.

2 | MATERIALS AND METHODS

2.1 | Patients

Patients with SESCO who underwent endoscopic submucosal dissection (ESD) at the National Cancer Center Hospital East, with histologically diagnosed negative horizontal and vertical margins, and with the pathological staging of pTis or pT1a between March 2019 and October 2019 and with the pathological staging of pT1b between September 2015 and October 2019, met the inclusion criteria of this study. Patients who had a history of chemotherapy and/or radiotherapy for esophageal and/or head and neck cancers were excluded from the study.

2.2 | Histopathologic examinations

Routine pathologic diagnoses of ESD specimens were performed as follows: Each ESD specimen was fixed in 10% neutral buffered formalin and cut into 2 mm slices, vertical to the long axis, and then processed for paraffin embedding and sectioning. Hematoxylin and eosin staining (H&E) was performed, and then the specimens were examined using light microscopy by two pathologists. The depth of invasion, lateral and deep margins, degree of differentiation, and lymphatic and vascular invasion were reported based on the Japanese Classification of Esophageal Cancer, and the T classification was categorized according to the guidelines of the 8th edition of the TNM classification.^{26,27}

2.3 | Immunohistochemical staining

Immunohistochemical staining was performed on the VENTANA BenchMark ULTRA automated slide stainer (VENTANA, Roche). The primary antibodies used in this study are listed in Table S1.

2.4 | Evaluation of the expression of HIF-1 α , CAIX, and GLUT1

The SESCC and the adjacent non-neoplastic esophageal epithelium, in one target section with the most widespread cancer cells in pTis-T1a or with the deepest depth of invasion by cancer cells in pT1b, together with the expression of HIF-1 α , CAIX, and GLUT1 were evaluated with immunohistochemical staining, and H-score assignment was performed by two pathologists.^{28–30} The staining intensity of HIF-1 α based on nuclear staining and that of CAIX and GLUT1 based on membrane staining was scored using the following classification system: [0], negative staining; [1+], weak staining; [2+], moderate staining; [3+], strong staining (Figure 1). Thus, the H-score was calculated as follows: 1 \times (the percentage of cancer cells staining [1+]) + 2 \times (the percentage of cancer cells staining [2+]) + 3 \times (the percentage of cancer cells staining [3+]).

2.5 | Evaluation of microvessel count (MVC) and microvessel density (MVD)

All slides were automatically scanned using the virtual slide scanner NanoZoomer (Hamamatsu Photonics) at 40 \times magnification after data anonymization and setting of image acquisition parameters. The total area of SESCC and adjacent non-neoplastic esophageal epithelium in one target section was selected, and the total number and area of blood vessels in SESCC and adjacent non-neoplastic esophageal epithelium, which were stained for both CD31 and α -smooth muscle actin (α -SMA), were measured. Further, the microvessel count (MVC) and microvessel density (MVD) were calculated by dividing the total number and area of blood vessels per total area of SESCC or adjacent non-neoplastic esophageal epithelium, respectively.^{31,32} Representative photomicrographs of double immunohistochemical staining for CD31 and α -SMA in SESCC are shown in Figure S1A,B.

2.6 | Oxygen saturation (StO₂) measurement using OXEI

As we previously reported, the mechanism for imaging the oxygen saturation (StO₂) with OXEI is to detect the difference in absorption coefficient between oxidized and reduced hemoglobin on the mucosal surface using two laser light

wavelengths (445 and 473 nm) and process the obtained images and transform it as StO₂ color maps.²³ The both images of ordinary white-light imaging and OXEI imaging with StO₂ color map can be synchronously captured and filed.

The entire SESCC in pTis-T1a or the deepest part of SESCC in pT1b, which was captured based on the pathological findings, and the adjacent non-neoplastic esophageal mucosa were selected with white-light endoscopic images by two endoscopists. OXEI was synchronized to each target area, and the StO₂ was quantified using the dedicated software. The StO₂ difference between SESCC and adjacent non-neoplastic esophageal mucosa in the same image was calculated as Δ StO₂. The method used to quantify the StO₂ and Δ StO₂ with the OXEI images is shown in Figure S2.

2.7 | Statistical analysis

Patient and lesion characteristics were summarized using proportion or descriptive statistics such as mean, median, and range. Comparison between groups was assessed by employing Mann–Whitney *U* test. The correlations between the expression of hypoxia markers and MVD were determined using Spearman's rank correlation coefficient. All *p* values were reported as two-sided, and *p* < 0.05 was considered statistically significant. All statistical analyses were performed with EZR (Saitama Medical Center, Jichi Medical University), a graphical user interface for R 4.1.0 (R Foundation for Statistical Computing). More precisely, EZR is a modified version of R commander (version 2.7-0) designed to add statistical functions frequently used in biostatistics.³³

3 | RESULTS

3.1 | Clinicopathological characteristics of patients and lesions in pathological studies

Of the 130 lesions from 121 patients, 109 lesions from 102 patients were enrolled and evaluated in this study (Figure S3). The pathological depths of invasion were pTis (36 lesions, 33%), pT1a (42 lesions, 39%), pT1b (31 lesions, 28%). The clinicopathological characteristics of the patients and lesions are presented in Table S2.

3.2 | The expression of hypoxia markers with immunohistochemical staining by the depth of invasion

The mean (range) H-score of HIF-1 α in non-neoplasia, pTis-T1a, and pT1b was 4.95 (0–60), 5.51 (0–60), and 16.0 (0–90), respectively. The mean (range) H-score of CAIX in

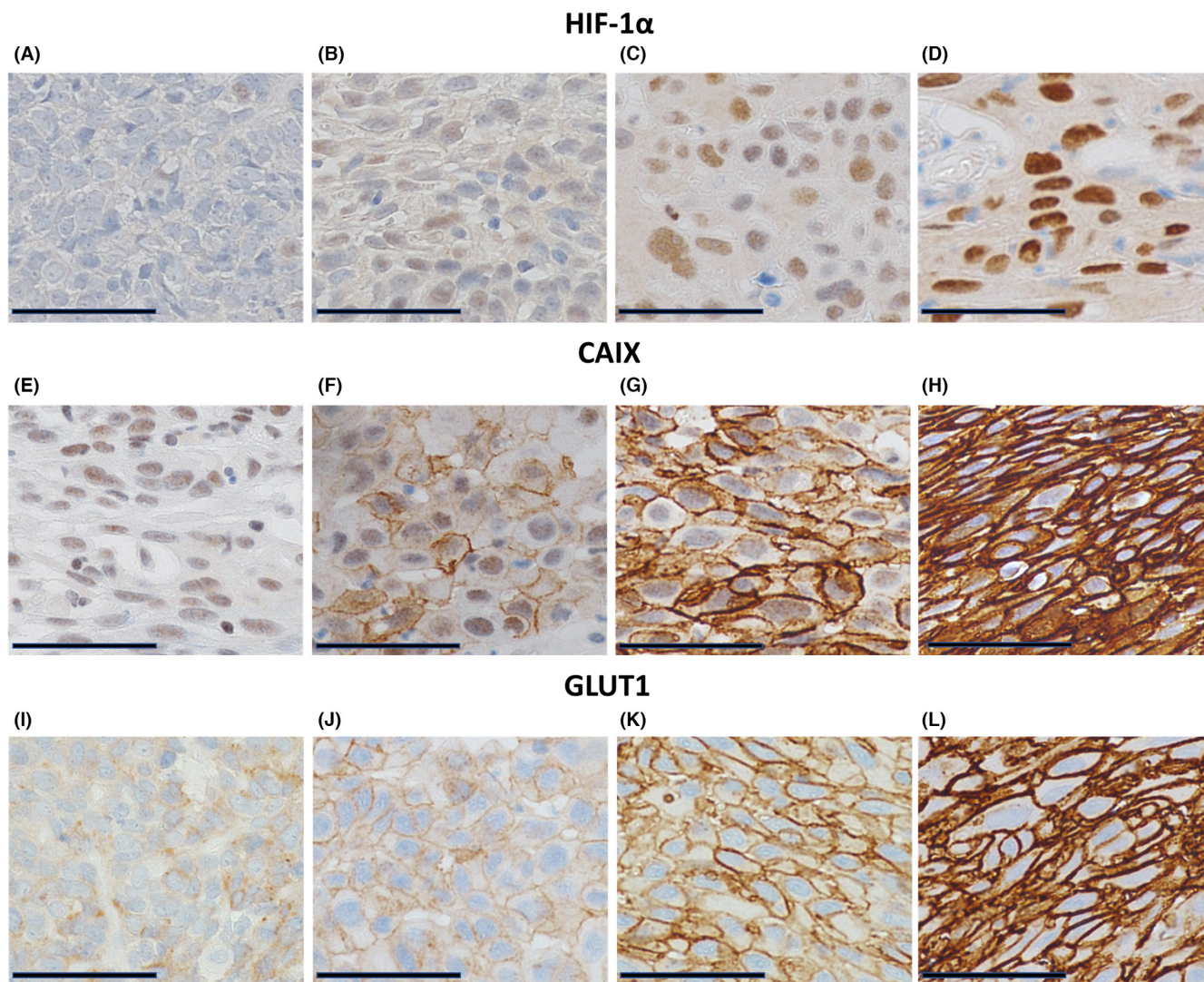


FIGURE 1 (A–L) Representative photomicrographs of immunohistochemical staining of HIF-1 α (A–D), CAIX (E–H), and GLUT1 (I–L). The intensity of staining was evaluated in the nuclei for HIF-1 α and in the membrane for CAIX and GLUT1. Scale Bar: 50 μ m. (A, E, I) 0, negative staining. (B, F, J) 1+, weak staining. (C, G, K) 2+, moderate staining. (D, H, L) 3+, strong staining.

non-neoplasia, pTis-T1a, and pT1b was 0.290 (0–3), 13.0 (0–170), and 15.6 (0–170), respectively. The mean (range) H-score of GLUT1 in non-neoplasia, pTis-T1a, and pT1b was 37.6 (0–160), 199 (70–300), and 177 (40–280), respectively. The expression of HIF-1 α was significantly higher in pT1b than in non-neoplasia ($p < 0.001$, Figure 2A) and in pT1b than in pTis-T1a ($p = 0.00472$, Figure 2A). The expression of CAIX and GLUT1 was significantly higher in SESCC than in non-neoplasia ($p < 0.001$, $p < 0.001$, respectively, Figure 2B,C).

3.3 | Evaluation of MVC and MVD by the depth of invasion and the relationship between them and the expression of hypoxia markers

The median (range) MVC in non-neoplasia, pTis-T1a, and pT1b was 14.2/ mm^2 (2.14–42.5/ mm^2), 22.7/ mm^2

(3.46–66.3/ mm^2), and 24.8/ mm^2 (11.8–48.1/ mm^2), respectively. MVC was significantly higher in SESCC than in non-neoplasia ($p < 0.001$, Figure 3A). The median (range) MVD in non-neoplasia, pTis-T1a, and pT1b was 0.478% (0.0391–2.24%), 0.991% (0.0639–7.09%), and 1.51% (0.447–8.80%), respectively. MVD was significantly higher in SESCC than in non-neoplasia ($p < 0.001$, Figure 3A) and in pT1b than in pTis-T1a ($p = 0.00479$, Figure 3A). Representative photomicrographs of MVC and MVD in non-neoplastic tissue, pTis, and pT1b are shown in Figure 3B. MVD was positively correlated with the expression of HIF-1 α , CAIX, and GLUT1 ($R = 0.24$, $R = 0.29$, $R = 0.52$, respectively, Figure 4A). Moreover, MVD was significantly increased in the positive expression group of HIF-1 α and CAIX compared with that in the negative expression group ($p = 0.00120$, $p < 0.001$, respectively, Figure 4B) and in the higher expression group of GLUT1 (H-score > 100) compared with that in

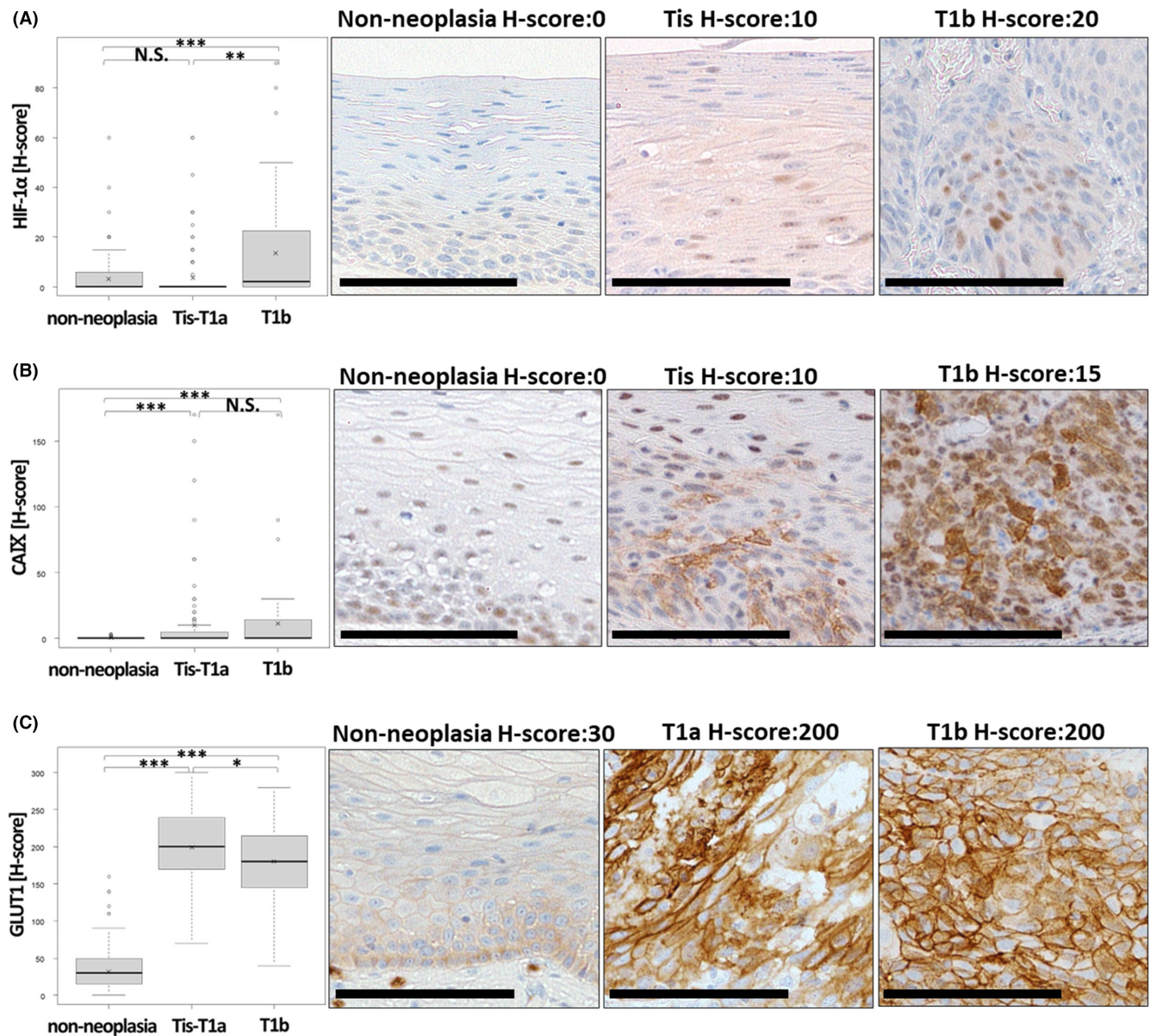


FIGURE 2 (A, B) Comparison of the expression of hypoxia markers in non-neoplasia ($n=109$), pTis-T1a ($n=78$), and pT1b ($n=31$). Additionally, representative photomicrographs of immunohistochemical staining of HIF-1 α (A), CAIX (B), and GLUT1 (C). N.S., not significant, * $p < 0.05$, ** $p < 0.01$, *** $p < 0.001$. Scale Bar: 100 μm .

the lower expression group (H-score ≤ 100) ($p < 0.001$, Figure 4B).

3.4 | Oxygen saturation (StO₂) quantified with OXEI by the depth of invasion

During the study period, we evaluated 16 consecutive lesions from 15 patients both with OXEI before ESD and pathological immunostainings of ESD specimens. The pathological depths of invasion were pTis (5 lesions, 31%), pT1a (6 lesions, 38%), pT1b (5 lesions, 31%). The median (range) StO₂ in non-neoplasia, pTis-T1a, and pT1b

was 61.5% (52%–80%), 62% (53%–75%), and 54% (51%–60%), respectively. The StO₂ was significantly lower in pT1b than in non-neoplasia ($p=0.00131$, Figure 5A) and tended to be lower in pT1b than in pTis-T1a ($p=0.0606$, Figure 5A). The median (range) ΔStO_2 in pTis-T1a and pT1b was -1% (-5% to $+3\%$) and -7% (-13% to -5%), respectively. ΔStO_2 was significantly lower in pT1b than in pTis-T1a ($p=0.00260$, Figure 5A). Images of the StO₂, quantified using OXEI, and photomicrographs of immunohistochemical staining of HIF-1 α , CAIX, and GLUT1 and double immunohistochemical staining of CD31 and $\alpha\text{-SMA}$ in a representative case of pT1b ESCC are shown in Figure 5B–F.

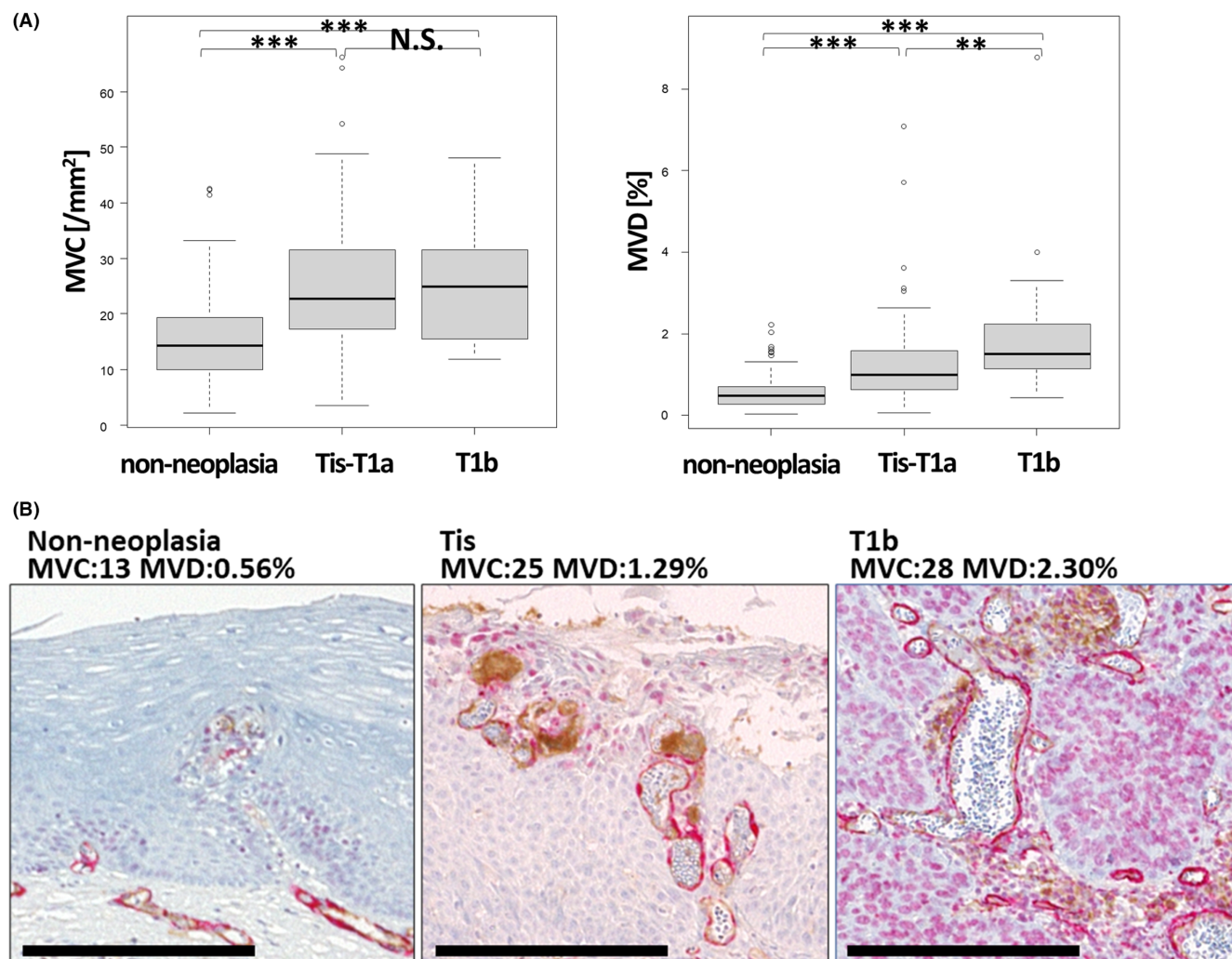


FIGURE 3 (A) Comparison of MVC and MVD in non-neoplasia ($n=109$), pTis-T1a ($n=78$), and pT1b ($n=31$). (B) Representative photomicrographs of MVC and MVD in non-neoplasia, pTis, and pT1b. N.S., not significant, ** $p < 0.01$, *** $p < 0.001$. Scale Bar: 500 μ m.

4 | DISCUSSION

In this study, two important results were obtained. First, the expression of all hypoxia markers and vessel density were significantly different in pT1b compared with those in non-neoplasia, whereas the expression of HIF-1 α was not significantly different in pTis-T1a compared with that in non-neoplasia. Second, the StO₂ in vivo with OXEI was significantly lower in pT1b than in non-neoplasia and tended to be lower in pT1b than in pTis-T1a, whereas it was not significantly different in pTis-T1a compared with in non-neoplasia. To the best of our knowledge, this was the first study to compare the expression of hypoxia markers, vessel density, and StO₂ in non-neoplasia, pTis-T1a, and pT1b with ESD specimens. These important results suggest that ESCC becomes markedly hypoxic in especially pT1b.

The strength of this study was the evaluation of the expression of hypoxia markers and vessel density in the

largest number of SESCC samples compared with that in previous reports^{18,34} and the inclusion of ESD specimens that were histologically diagnosed as having negative horizontal and vertical margins, excluding surgical specimens, in order to evaluate them under certain conditions. No previous study has examined in detail the oxygen status of SESCC in a large number of cases using only ESD specimens. The expression of hypoxia markers and vessel density were similar as in previous reports, indicating that in ESCC, they become higher as tumor invades deeper.^{10,12–18,35} When examined in detail, the expression of all hypoxia markers and vessel density were significantly different in pT1b compared with those in non-neoplasia, whereas the expression of HIF-1 α was not significantly different in pTis-T1a compared with that in non-neoplasia, which is a novel finding. In the present study, vessel density was higher in T1b than in pTis-T1a, suggesting more progressive angiogenesis, similar to previous reports.¹⁸ It has also been previously reported that the expression of

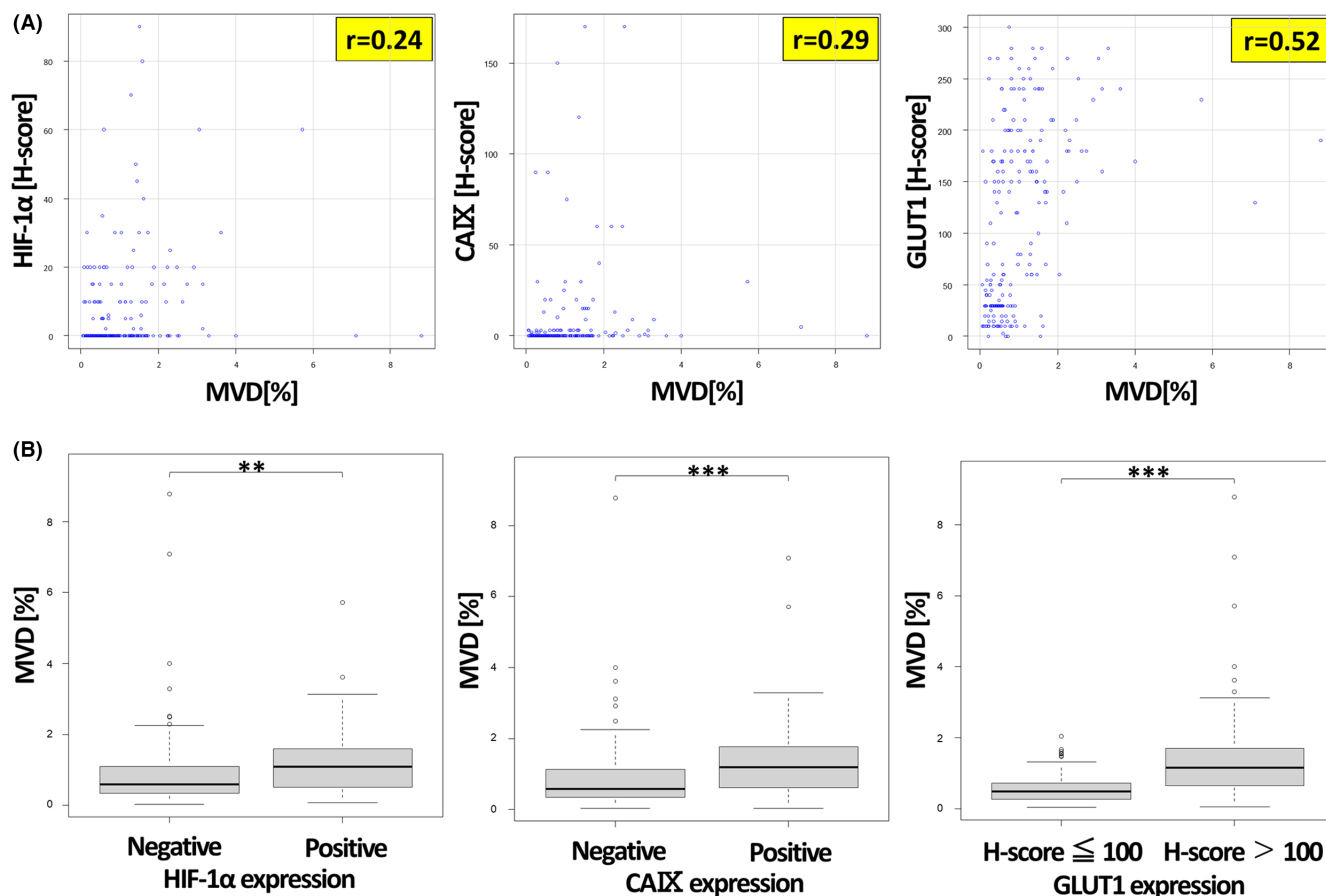


FIGURE 4 (A) Correlation between MVD and the expression of hypoxia markers in non-neoplasia and SESCC ($n=218$). MVD was positively correlated with the expression of HIF-1 α , CAIX, and GLUT1. (B) MVD was significantly higher in the positive expression group of HIF-1 α and CAIX than in the negative expression group, and MVD was significantly increased in the higher expression group of GLUT1 (H-score > 100) compared with that in the lower expression group of GLUT1 (H-score \leq 100). ** $p < 0.01$, *** $p < 0.001$.

HIF-1 α is higher as angiogenesis progresses.^{10,16} These findings suggest that the expression of all hypoxia markers and vessel density are significantly different in pT1b compared to non-neoplasia as the oxygen environment becomes hypoxic, caused by the progression of angiogenesis. As a result of less advanced angiogenesis in pTis-T1a compared to pT1b, the expression of HIF-1 α is almost negligible, suggesting that the oxygen environment in pTis-T1a may be closer to normoxia than in pT1b.

Further, the strength of this study is that OXEI allowed us to evaluate StO₂ more safely, in real time, than other methods of evaluating StO₂. The gold standard method for the quantification of the StO₂ is the direct measurement of StO₂ in the tumor using an Eppendorf needle electrode system, but this method is highly invasive because the electrode is directly inserted into the tumor.^{36,37} PET-based hypoxia imaging with probes such as 18F-FMISO,³⁸ 60 and 64Cu-ATSM,^{39,40} and 18F-FAZA⁴¹ has been reported as a method for non-invasive estimation of StO₂, but it has the disadvantage of being affected by drug metabolism and the need to prepare an expensive device. And it must

be hard to detect and measure StO₂ of superficial cancer in digestive tract with PET. OXEI is an image-enhanced digestive tract endoscopy that can show StO₂ in vivo, in real time, on digestive tract lesions including SESCC. Similar to ordinary endoscopic observation, OXEI can safely image StO₂ without puncture and drug administration. In this study, StO₂ was not significantly different in pTis-T1a compared to non-neoplasia, but was significantly lower in pT1b than in non-neoplasia and tended to be lower in pT1b than in pTis-T1a, which is a novel finding. The oxygen environment quantified using the Eppendorf needle electrode system and PET has been reported to be hypoxic in some solid tumors compared to non-neoplasia, and the oxygen environment becomes more hypoxic as they progress.^{23,36–41} In a previous study, Kaneko et al.²³ reported that the StO₂ in vivo with OXEI was significantly lower in esophageal neoplasia than in non-neoplasia, but it is not known whether StO₂ was lower in pTis-T1a or pT1b. Our StO₂ findings suggest that the oxygen environment is markedly hypoxic in T1b, while it is close to normoxia in pTis-T1a.

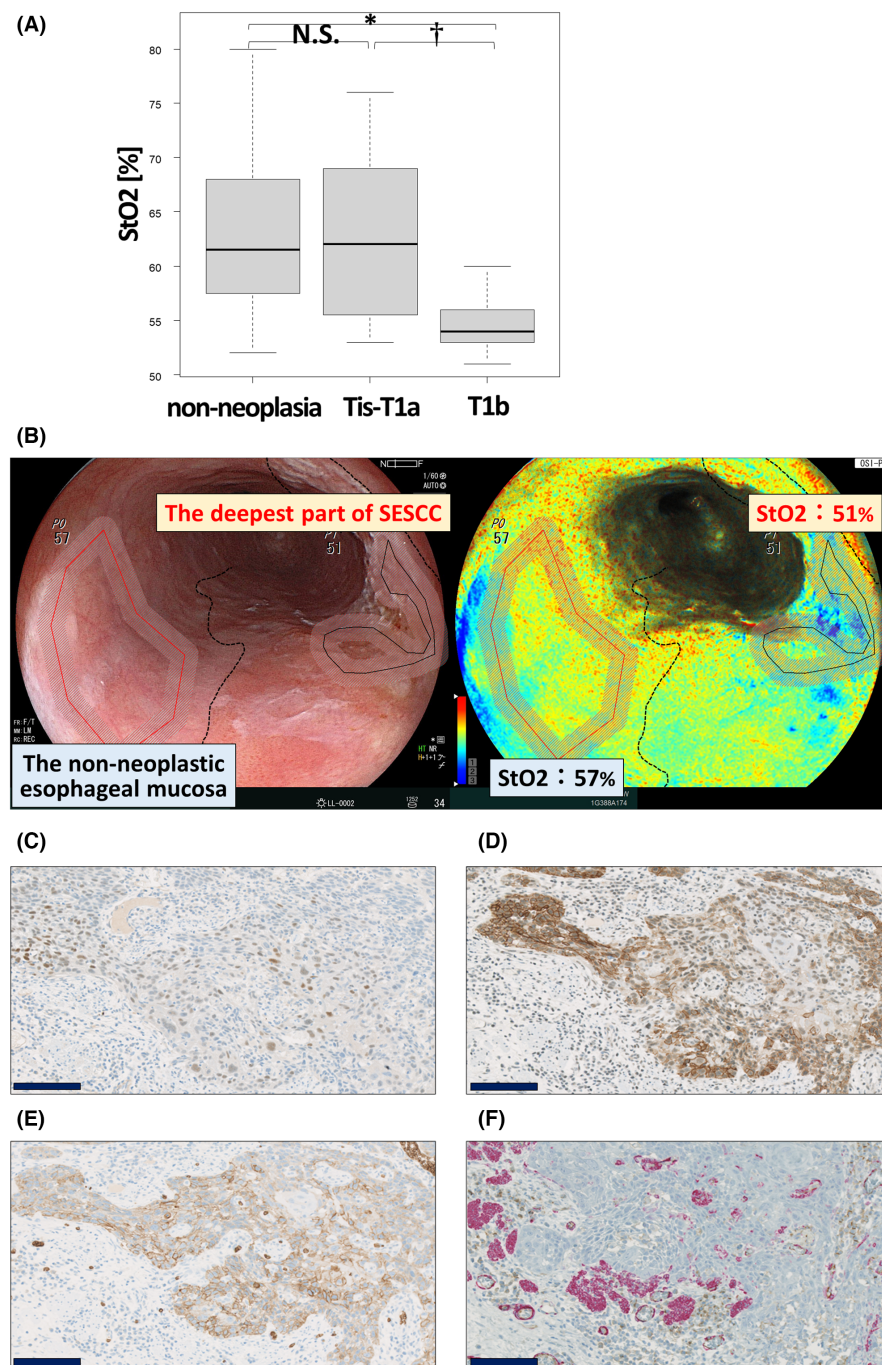


FIGURE 5 (A) Comparison of StO₂ in non-neoplasia ($n = 16$), pTis-T1a ($n = 11$), and pT1b ($n = 5$). N.S., not significant, † $p < 0.1$, * $p < 0.05$. (B–E) Representative photomicrographs of StO₂ quantified with OXEI (B), immunohistochemical staining of HIF-1 α (C), CAIX (D), and GLUT1 (E), and double immunohistochemical staining of CD31 and α -SMA (F). The StO₂ in the deepest part of this T1b ESCC was 51% and in this adjacent non-neoplastic esophageal mucosa was 57%, and Δ StO₂ was -6% . Scale Bar: 100 μ m.

These important results, confirmed by immunohistochemical staining and OXEI, suggest that ESCC becomes markedly hypoxic in pT1b and it may be close to normoxia in Tis-T1a. This is significant because it clarifies the biological characteristics of the oxygen environment in SESCC. Clinically, pT1b ESCC is markedly more metastatic and has a poorer prognosis than pTis-T1a.⁴² The present results suggest that factors associated with metastasis may be associated with changes in the oxygen status in SESCC. This may lead to elucidation of the biological mechanisms involved in the malignant transformation associated with submucosal invasion of SESCC. Additionally, OXEI may be useful

for the prediction of the depth of invasion between pTis-T1a and pT1b. Actually, Δ StO₂ was less than -5 in 1 out of 11 cases with pTis-T1a and in 5 out of 5 cases for pT1b, and Δ StO₂ was significantly lower in pT1b than in pTis-T1a (Figure S4). In SESCC, the prediction of the depth of invasion is important because the treatment strategy differs between pTis-T1a and pT1b.⁴³ One of the imaging methods used to predict the depth of invasion in SESCC is the evaluation of blood vessel morphology by magnifying endoscopy, using narrowband imaging, but its diagnostic capability is not yet sufficient.^{43,44} This result indicates that Δ StO₂ may be more useful in the prediction of the depth of invasion.

There are some limitations to this study. First, this study was a retrospective study, and we collected as many images as possible, but the number of OXEI cases was small. We are currently collecting the OXEI images of digestive tract lesions including ESCC and hope to investigate larger number of cases in the future. Second, the endoscopically resected specimens included in this study were limited to shallow pT1b ESCC cases that were preoperatively judged to be endoscopically treatable lesions up to the clinical T1b-SM1. In order to solve this problem, it may be necessary to examine deep pT1b ESCC including the clinical T1b-SM2/3 with surgery. However, endoscopic and surgical resection may each have different effects on the expression of hypoxia markers and vessel density due to the differences in the procedure of blood flow blockade from major vessels.

In summary, current results suggest that ESCC becomes hypoxic with high vessel density even at an early stage. This is especially prominent in T1b. As the number of cases evaluated with OXEI in this study was small, we would like to increase the number of cases in the future for further studies.

AUTHOR CONTRIBUTIONS

Nobuhisa Minakata: Conceptualization (equal); data curation (lead); formal analysis (equal); funding acquisition (lead); investigation (lead); methodology (equal); project administration (equal); resources (equal); software (equal); visualization (lead); writing – original draft (lead). **Shingo Sakashita:** Conceptualization (lead); methodology (lead); project administration (equal); supervision (equal); writing – original draft (equal); writing – review and editing (equal). **Masashi Wakabayashi:** Formal analysis (lead); methodology (supporting); writing – review and editing (supporting). **Yuka Nakamura:** Resources (lead); software (lead). **Hironori Sunakawa:** Conceptualization (equal); funding acquisition (equal); supervision (equal); writing – original draft (supporting); writing – review and editing (supporting). **Yusuke Yoda:** Conceptualization (equal). **Genichiro Ishii:** Conceptualization (equal); methodology (equal); writing – review and editing (lead). **Tomonori Yano:** Conceptualization (equal); funding acquisition (equal); project administration (lead); supervision (lead); writing – review and editing (equal).

ACKNOWLEDGMENTS

This work was supported by the donation from the Center of New Surgical and Endoscopic Development for Exploratory Technology and JSPS KAKENHI Grant Numbers JP20K22859, and JP21K06899. A part of this study is supported by the National Cancer Center Research and Development Fund (2020-A-10).

CONFLICT OF INTEREST STATEMENT

Tomonori Yano received a research grant from Fujifilm Corporation. The Oxygen saturation imaging system is provided by FUJIFILM under research construction. All authors had full access to all the data in the study and are in agreement with the decision to submit this publication; Nobuhisa Minakata, Shingo Sakashita, Masashi Wakabayashi, Yuka Nakamura, Hironori Sunakawa, Yusuke Yoda, and Genichiro Ishii have no conflicts of interest.

DATA AVAILABILITY STATEMENT

Not Available.

ETHICS STATEMENT

Approval of the research protocol by an Institutional Reviewer Board: This study has been approved by the Institutional Review Board of the National Cancer Center (2020–361).

ORCID

Nobuhisa Minakata  <https://orcid.org/0000-0003-4540-4036>

REFERENCES

- Vaupel P, Kallinowski F, Okunieff P. Blood flow, oxygen and nutrient supply, and metabolic microenvironment of human tumors: a review. *Cancer Res.* 1989;49(23):6449-6465.
- Carmeliet P, Jain RK. Principles and mechanisms of vessel normalization for cancer and other angiogenic diseases. *Nat Rev Drug Discov.* 2011;10(6):417-427. doi:10.1038/nrd3455
- Harris AL. Hypoxia—a key regulatory factor in tumour growth. *Nat Rev Cancer.* 2002;2(1):38-47. doi:10.1038/nrc704
- Wykoff CC, Beasley NJ, Watson PH, et al. Hypoxia-inducible expression of tumor-associated carbonic anhydrases. *Cancer Res.* 2000;60(24):7075-7083.
- Chen C, Pore N, Behrooz A, Ismail-Beigi F, Maity A. Regulation of glut1 mRNA by hypoxia-inducible factor-1. Interaction between H-ras and hypoxia. *J Biol Chem.* 2001;276(12):9519-9525. doi:10.1074/jbc.M010144200
- Ema M, Taya S, Yokotani N, Sogawa K, Matsuda Y, Fujii-Kuriyama Y. A novel bHLH-PAS factor with close sequence similarity to hypoxia-inducible factor 1alpha regulates the VEGF expression and is potentially involved in lung and vascular development. *Proc Natl Acad Sci U S A.* 1997;94(9):4273-4278. doi:10.1073/pnas.94.9.4273
- Carmeliet P, Dor Y, Herbert JM, et al. Role of HIF-1alpha in hypoxia-mediated apoptosis, cell proliferation and tumour angiogenesis. *Nature.* 1998;394(6692):485-490. doi:10.1038/28867
- Semenza GL. Targeting HIF-1 for cancer therapy. *Nat Rev Cancer.* 2003;3(10):721-732. doi:10.1038/nrc1187
- Takala H, Saarnio J, Wiik H, Ohtonen P, Soini Y. HIF-1 α and VEGF are associated with disease progression in esophageal carcinoma. *J Surg Res.* 2011;167(1):41-48. doi:10.1016/j.jss.2009.11.725

10. Kimura S, Kitadai Y, Tanaka S, et al. Expression of hypoxia-inducible factor (HIF)-1 α is associated with vascular endothelial growth factor expression and tumour angiogenesis in human oesophageal squamous cell carcinoma. *Eur J Cancer*. 2004;40(12):1904-1912. doi:10.1016/j.ejca.2004.04.035
11. Sung H, Ferlay J, Siegel RL, et al. Global cancer statistics 2020: GLOBOCAN estimates of incidence and mortality worldwide for 36 cancers in 185 countries. *CA A Cancer J Clin*. 2021;71(3):209-249. doi:10.3322/caac.21660
12. van Kuijk SJA, Yaromina A, Houben R, Niemans R, Lambin P, Dubois LJ. Prognostic significance of carbonic anhydrase IX expression in cancer patients: a meta-analysis. *Front Oncol*. 2016;6:69. doi:10.3389/fonc.2016.00069
13. Tanaka N, Kato H, Inose T, et al. Expression of carbonic anhydrase 9, a potential intrinsic marker of hypoxia, is associated with poor prognosis in oesophageal squamous cell carcinoma. *Br J Cancer*. 2008;99(9):1468-1475. doi:10.1038/sj.bjc.6604719
14. Sawayama H, Ishimoto T, Watanabe M, et al. High expression of glucose transporter 1 on primary lesions of esophageal squamous cell carcinoma is associated with hematogenous recurrence. *Ann Surg Oncol*. 2014;21(5):1756-1762. doi:10.1245/s10434-013-3371-1
15. Kurokawa T, Miyamoto M, Kato K, et al. Overexpression of hypoxia-inducible-factor 1 α (HIF-1 α) in oesophageal squamous cell carcinoma correlates with lymph node metastasis and pathologic stage. *Br J Cancer*. 2003;89(6):1042-1047. doi:10.1038/sj.bjc.6601186
16. Shao JB, Li Z, Zhang N, Yang F, Gao W, Sun ZG. Hypoxia-inducible factor 1 α in combination with vascular endothelial growth factor could predict the prognosis of postoperative patients with oesophageal squamous cell cancer. *Pol J Pathol*. 2019;70(2):84-90. doi:10.5114/pjp.2019.87100
17. Sun G, Hu W, Lu Y, Wang Y. A meta-analysis of HIF-1 α and esophageal squamous cell carcinoma (ESCC) risk. *Pathol Oncol Res*. 2013;19(4):685-693. doi:10.1007/s12253-013-9631-3
18. Kumagai Y, Sobajima J, Higashi M, et al. Angiogenesis in superficial esophageal squamous cell carcinoma: assessment of microvessel density based on immunostaining for CD34 and CD105. *Jpn J Clin Oncol*. 2014;44(6):526-533. doi:10.1093/jjco/hyu039
19. Kuwano H, Sonoda K, Yasuda M, Sumiyoshi K, Nozoe T, Sugimachi K. Tumor invasion and angiogenesis in early esophageal squamous cell carcinoma. *J Surg Oncol*. 1997;65(3):188-193. doi:10.1002/(sici)1096-9098(199707)65:3<188::aid-jso8>3.0.co;2-2
20. Talks KL, Turley H, Gatter KC, et al. The expression and distribution of the hypoxia-inducible factors HIF-1 α and HIF-2 α in normal human tissues, cancers, and tumor-associated macrophages. *Am J Pathol*. 2000;157(2):411-421. doi:10.1016/s0002-9440(10)64554-3
21. Turner JR, Odze RD, Crum CP, Resnick MB. MN antigen expression in normal, preneoplastic, and neoplastic esophagus: a clinicopathological study of a new cancer-associated biomarker. *Hum Pathol*. 1997;28(6):740-744. doi:10.1016/s0046-8177(97)90185-4
22. Zhao X, Huang Q, Koller M, et al. Identification and validation of esophageal squamous cell carcinoma targets for fluorescence molecular endoscopy. *Int J Mol Sci*. 2021;22(17):9270. doi:10.3390/ijms22179270
23. Kaneko K, Yamaguchi H, Saito T, et al. Hypoxia imaging endoscopy equipped with laser light source from preclinical live animal study to first-in-human subject research. *PLOS One*. 2014;9(6):e99055. doi:10.1371/journal.pone.0099055
24. Nishihara K, Hori K, Saito T, et al. A study of evaluating specific tissue oxygen saturation values of gastrointestinal tumors by removing adherent substances in oxygen saturation imaging. *PLOS One*. 2021;16(1):e0243165. doi:10.1371/journal.pone.0243165
25. Suyama M, Yoda Y, Yamamoto Y, et al. Oxygen saturation imaging as a useful tool for visualizing the mode of action of photodynamic therapy for esophageal cancer. *VideoGIE*. 2020;5(10):496-499. doi:10.1016/j.vgie.2020.07.003
26. The Japan Esophageal Society. *Japanese Classification of Esophageal Cancer*. 11th ed. Tokyo, Japan: Kanehara & Co., LTD.; 2015.
27. Brierley JD, Gospodarowicz MK, Wittekind C. *TNM classification of malignant tumours*. 8th ed. Chichester: John Wiley & Sons; 2017.
28. Hirsch FR, Varella-Garcia M, Bunn PA, et al. Epidermal growth factor receptor in non-small-cell lung carcinomas: correlation between gene copy number and protein expression and impact on prognosis. *J Clin Oncol*. 2003;21(20):3798-3807. doi:10.1200/JCO.2003.11.069
29. Pirker R, Pereira JR, von Pawel J, et al. EGFR expression as a predictor of survival for first-line chemotherapy plus cetuximab in patients with advanced non-small-cell lung cancer: analysis of data from the phase 3 FLEX study. *Lancet Oncol*. 2012;13(1):33-42. doi:10.1016/S1470-2045(11)70318-7
30. Mazières J, Brugger W, Cappuzzo F, et al. Evaluation of EGFR protein expression by immunohistochemistry using H-score and the magnification rule: re-analysis of the SATURN study. *Lung Cancer*. 2013;82(2):231-237. doi:10.1016/j.lungcan.2013.07.016
31. Patten SG, Adamcic U, Lacombe K, Minhas K, Skowronski K, Coomber BL. VEGFR2 heterogeneity and response to anti-angiogenic low dose metronomic cyclophosphamide treatment. *BMC Cancer*. 2010;10:683. doi:10.1186/1471-2407-10-683
32. Arimoto A, Uehara K, Tsuzuki T, Aiba T, Ebata T, Nagino M. Role of bevacizumab in neoadjuvant chemotherapy and its influence on microvessel density in rectal cancer. *Int J Clin Oncol*. 2015;20(5):935-942. doi:10.1007/s10147-015-0818-3
33. Kanda Y. Investigation of the freely available easy-to-use software "EZR" for medical statistics. *Bone Marrow Transplant*. 2013;48(3):452-458. doi:10.1038/bmt.2012.244
34. Ogane N, Yasuda M, Shimizu M, et al. Clinicopathological implications of expressions of hypoxia-related molecules in esophageal superficial squamous cell carcinoma. *Ann Diagn Pathol*. 2010;14(1):23-29. doi:10.1016/j.anndiagpath.2009.10.003
35. Elpek GO, Gelen T, Aksoy NH, et al. The prognostic relevance of angiogenesis and mast cells in squamous cell carcinoma of the oesophagus. *J Clin Pathol*. 2001;54(12):940-944. doi:10.1136/jcp.54.12.940
36. Brown JM, Wilson WR. Exploiting tumour hypoxia in cancer treatment. *Nat Rev Cancer*. 2004;4(6):437-447. doi:10.1038/nrc1367
37. Höckel M, Vaupel P. Tumor hypoxia: definitions and current clinical, biologic, and molecular aspects. *J Natl Cancer Inst*. 2001;93(4):266-276. doi:10.1093/jnci/93.4.266

38. Koh W-J, Rasey JS, Evans ML, et al. Imaging of hypoxia in human tumors with [F-18]fluoromisonidazole. *Int J Radiat Oncol Biol Phys.* 1992;22:199-212.
39. Lewis JS, Laforest R, Dehdashti F, Grigsby PW, Welch MJ, Siegel BA. An imaging comparison of 64Cu-ATSM and 60Cu-ATSM in cancer of the uterine cervix. *J Nucl Med.* 2008;49(7):1177-1182. doi:10.2967/jnumed.108.051326
40. Dehdashti F, Grigsby PW, Lewis JS, Laforest R, Siegel BA, Welch MJ. Assessing tumor hypoxia in cervical cancer by PET with 60Cu-labeled diacetyl-bis(N4-methylthiosemicarbazone). *J Nucl Med.* 2008;49(2):201-205. doi:10.2967/jnumed.107.048520
41. Servagi-Vernat S, Differding S, Hanin FX, et al. A prospective clinical study of ¹⁸F-FAZA PET-CT hypoxia imaging in head and neck squamous cell carcinoma before and during radiation therapy. *Eur J Nucl Med Mol Imaging.* 2014;41(8):1544-1552. doi:10.1007/s00259-014-2730-x
42. Oyama T, Miyata Y, Shimatani S, et al. Lymph nodal metastasis of m3, sm1 esophageal cancer. *Stom Intest.* 2002;37(1):71-74. doi:10.11477/mf.1403103406
43. Ishihara R, Arima M, Iizuka T, et al. Endoscopic submucosal dissection/endoscopic mucosal resection guidelines for esophageal cancer. *Dig Endosc.* 2020;32(4):452-493. doi:10.1111/den.13654
44. Oyama T, Inoue H, Arima M, et al. Prediction of the invasion depth of superficial squamous cell carcinoma based on microvessel morphology: magnifying endoscopic classification of the Japan Esophageal Society. *Esophagus.* 2017;14(2):105-112. doi:10.1007/s10388-016-0527-7

SUPPORTING INFORMATION

Additional supporting information can be found online in the Supporting Information section at the end of this article.

How to cite this article: Minakata N, Sakashita S, Wakabayashi M, et al. Immunohistochemistry and oxygen saturation endoscopic imaging reveal hypoxia in submucosal invasive esophageal squamous cell carcinoma. *Cancer Med.* 2023;12: 15809-15819. doi:10.1002/cam4.6217